MOTOR YACHT HULL FORM DESIGN FOR THE DISPLACEMENT TO SEMI-DISPLACEMENT SPEED RANGE

Perry van Oossanen[1], Justus Heimann[2], Juryk Henrichs[3], Karsten Hochkirch[4]

[1] Naval Architect, Van Oossanen & Associates bv, Costerweg 1F, 6702AA, Wageningen, the Netherlands
[2] Head of Hydrodynamics, FutureShip GmbH, Benzstr. 2, D-14482 Potsdam, Germany
[3] Hydrodynamicist, Van Oossanen & Associates bv, Costerweg 1F, 6702AA, Wageningen, the Netherlands
[4] Vice President Fluid Engineering, FutureShip GmbH, Benzstr. 2, D-14482 Potsdam, Germany

ABSTRACT

Nowadays, the design of luxury motor yachts is focussed on ever higher speeds. Froude numbers between 0.6 and 0.8 are no longer an exception. The typical load profile of a motor yacht often consists of long range cruising at low speeds and only short periods of time at higher and maximum speeds. This indicates the need for focussing hull design over the entire speed range rather than on maximum speed only. For this purpose the concept of the Fast Displacement Hull Form (FDHF) is introduced.

The concept and the use of design features that have a large effect on the resistance over the speed range, such as the area of the immersed transom, bulbous bows, trim control and spray rails are discussed. A design methodology using a formal optimization method for the bulbous bow is described and it is shown that bulbous bows are also effective in the semi-displacement speed range.

A comparison of the FDHF concept, in terms of resistance, with model tests of displacement and semi-displacement motor yachts, shows a significant resistance improvement over the entire speed range, but especially at displacement speeds when comparing to semi-displacement hull forms. Issues such as stability, interior space and building cost are addressed.

NOMENCLATURE

C_P	Prismatic Coefficient	GM	Metacentric height
C_{TL}	Telfer Coefficient	L_{WL}	Length on the water line in m
Δ	Displacement in tonne	R_T	Total resistance in kN
$F_{N,L}$	Froude number	V	Speed in m/s
$F_{N,T}$	Froude number on transom immersion	T_T	Draught of immersed transom in m
$F_{N,V}$	Volumetric Froude number		

1. INTRODUCTION

In recent years, the design of luxury motor yachts is focussed on ever higher speeds. Design briefs often state speeds that would require traditional “displacement”-type motor yachts to be pushed over the hull speed into, or just over, the primary resistance hump. For a typical motor yacht of 40 to 50 meters, speeds of between 18 and 22 knots (corresponding to Froude numbers of 0.45 to 0.6) are no longer an exception. For many semi-displacement motor yachts, speeds are typically between 25 and 30 knots, or Froude numbers of about 0.6 to 0.85.

Once the yacht is launched and trials have been carried out, most of these yachts hardly ever run at top speed, but mostly operate at a cruising speed of around 12 or 13 knots (Froude numbers of about 0.3 to 0.35), as this is the most convenient speed for the guests and crew on board and assures the largest range. Obviously, a hull well designed for a speed of 20 or 25 knots is often not very efficient in running 12 or 13 knots. This indicates that a hull form purely designed for the maximum speed is not economical. The behaviour and performance of the yacht at cruising speed should also be taken into account.

The authors have carried out experiments for a large number of displacement and semi-displacement hull forms, for a variety of renowned yards and design offices, as well as private clients, both in the towing tank and with Computational Fluid Dynamics (CFD) software.

From these experiments and calculations it can be concluded that there are merits in deviating from a "traditional" displacement or semi-displacement hull form, to a hybrid concept, here entitled the "Fast Displacement Hull Form".

2. FAST DISPLACEMENT HULL FORM

The Fast Displacement Hull Form (FDHF), as developed by Van Oossanen & Associates bv (VOA), is aimed at semi-displacement yachts that need to achieve a good over-all performance, with respect to resistance, seakeeping and manoeuvring, rather than achieving optimum performance at maximum speed. Typically, this will apply to vessels with a large variation in load profile, e.g. as is the case for a luxury motor yacht: long cruises at an economical speed, mid-range cruising at a higher speed and the occasional sprint. The novel FDHF concept is aimed at obtaining resistance values at semi-displacement speeds that are comparable to (or better than) well-designed conventional semi-displacement vessels, and at obtaining favourable resistance values over the lower speed range, especially around the cruising speed, resulting in an improved economic efficiency and less environmental impact in terms of engine-emissions. A number of yachts have already been built with some features of this concept, resulting in good, well-performing and pleasantly behaving vessels, over the entire speed range.

3. SEMI-DISPLACEMENT HULL FORMS

3.1 Resistance Data Comparison

In order to compare the resistance of various types of hull forms of various lengths and displacements, a number of presentation methods are available. The so-called Telfer Coefficient (Telfer 1963), C_{TL}, is considered to be a convenient method. C_{TL} is here defined by Eq. 1 and typical C_{TL}-curves for various hull forms are plotted in Fig. 1 on the basis of $F_{N,L}$.

$$C_{TL} = \frac{R_T/\Delta}{\left(V/\sqrt{L_{WL}}\right)^2} = \frac{R_T \cdot L_{WL}}{\Delta \cdot V^2} \qquad (1)$$

Figure 1 shows a typical displacement hull form (round bilge, bulbous bow, small immersed transom area) to have the lowest relative resistance at lower Froude numbers. With increasing speed, this rapidly changes when the primary hump in the resistance curve around the hull speed is met (around $F_{N,L} \approx 0.40 \sim 0.45$). The semi-displacement hull form is average in resistance at lower speeds and best up to the fully-planing speed regime (the crossover is here assumed to be at $F_{N,L} \approx 1.0$). $F_{N,L}$ is defined by Eq. 2:

$$F_{N,L} = \frac{V}{\sqrt{g \cdot L_{WL}}} \qquad (2)$$

3.2 Round Bilge vs. Hard Chine

Significant research has been carried out regarding the advantages and disadvantages of round bilge and hard chine hull forms. Perhaps the most notable of these have been carried out by Bailey (1974) and Blount (1995 and 2009).

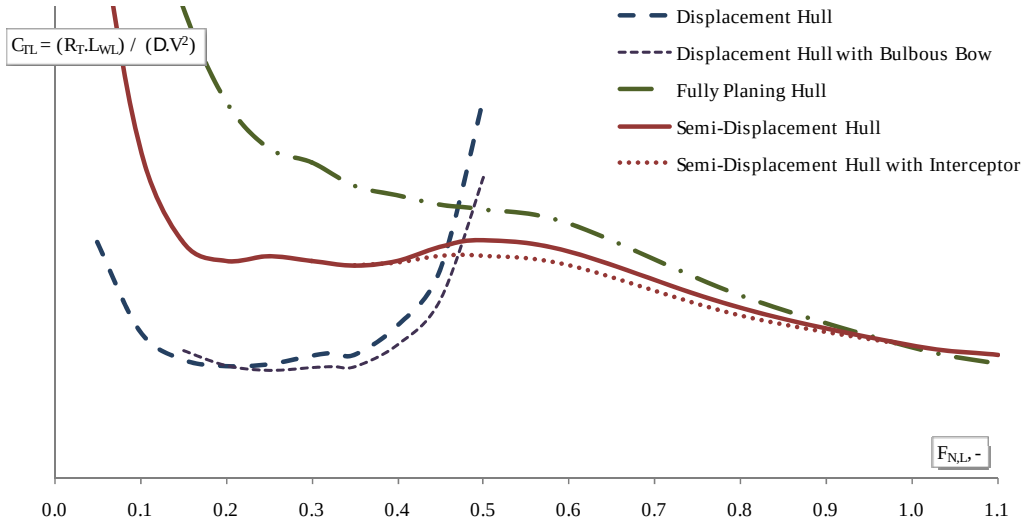

Fig. 1. Typical curves of C_{TL} for a displacement hull (with and without bulbous bow), a semi-displacement hard chine hull (with and without interceptor) and a fully planing hard chine hull.

From a calm-water resistance point of view, Blount (1995 and 2009) shows that hard chine hulls are to be preferred for values of $F_{N,L} > 0.75$. This conclusion is drawn from a comparison of a large number of model series, where the NPL series (Bailey 1976) stands out from a resistance point of view.

From a seakeeping point of view, round bilge hulls are supposed to be superior at displacement speeds, but at semi-displacement speeds there is no consensus about the superiority of round bilge or hard chine hulls (Blount 1995). This same conclusion is drawn by e.g. Keuning (1984). These publications, as well as research carried out by VOA, indicate that the influence of hull dimensions and parameters, such as slenderness ratio, length to beam ratio etc. have a far more significant influence on seakeeping than the actual section shape.

Furthermore, Blount (1995 and 2009) indicates that hard chine hulls are favourable with respect to dynamic stability and course-keeping at semi-displacement speeds. Bailey (1974) gives minimum values of *GM* for the NPL series in order to avoid loss of transverse stability at higher speeds, dependent on the beam-draft ratio.

A centreline skeg is necessary for a round bilge hull to ensure good course keeping stability and bilge keels and stabiliser fins are required to improve roll behaviour. It is to be noted that on displacement and semi-displacement yacht hulls, whether hard chine or round bilge, a centreline skeg is usually present, not just for course keeping, but also for docking the hull and protection of propellers and rudders. Stabiliser fins, for the purpose of stabilization at anchor, are also a standard feature on yachts, both for hard chine and round bilge hulls.

Considering the above, a round bilge hull has been adopted for the Fast Displacement Hull Form, with especially the improved resistance and seakeeping behaviour at displacement speeds in mind. Bilge keels need to be used but, assuming they are well-designed and aligned with the flow, these have a small penalty in resistance and are of easy construction.

3.3 Transom Area and LCG

Semi-displacement yachts often have a large immersed transom area (typically around 50 to 80% of the maximum sectional area) combined with a relatively aft location of *LCG*. A large transom area (and shallow buttocks) is usually applied in order to generate sufficient upwards pressure on the aft part of the hull, therewith reducing the running trim angle. A more level attitude of the hull, especially around the primary resistance hump and at the lower end of the semi-displacement speed range, reduces resistance significantly.

From experience and literature it is known that a submerged transom will not run dry up to $F_{N,T}$ values of about 2.5 to 3 (e.g. Doctors 2006), where $F_{N,T}$ is the Froude number based on transom immersion, see Eq. 3:

$$F_{N,T} = \frac{V}{\sqrt{g \cdot T_T}} \tag{3}$$

For yachts of around 40 to 50 metres this means that, at the denoted cruising speed of the yacht, typically around 12 or 13 knots ($F_{N,L} \approx 0.35$), the transom is often not yet completely dry and the associated drag constitutes a large portion of the total resistance of the yacht at that speed.

In Fig. 2, C_{TL} is plotted on the basis of the immersed transom area relative to the maximum sectional area for a number of displacement and semi-displacement hull forms, for $F_{N,L} = 0.35$ and 0.60. In this figure it can be seen that transom area is a very dominant factor in the resistance at $F_{N,L} = 0.35$ but that at $F_{N,L} = 0.60$ there is no dependency of resistance on the transom immersion.

Considering the above, the Fast Displacement Hull Form concept has a small immersed transom area (around 20 or 30% of the maximum sectional area). To ensure sufficient upward lift at higher speeds a (retractable) interceptor is used.

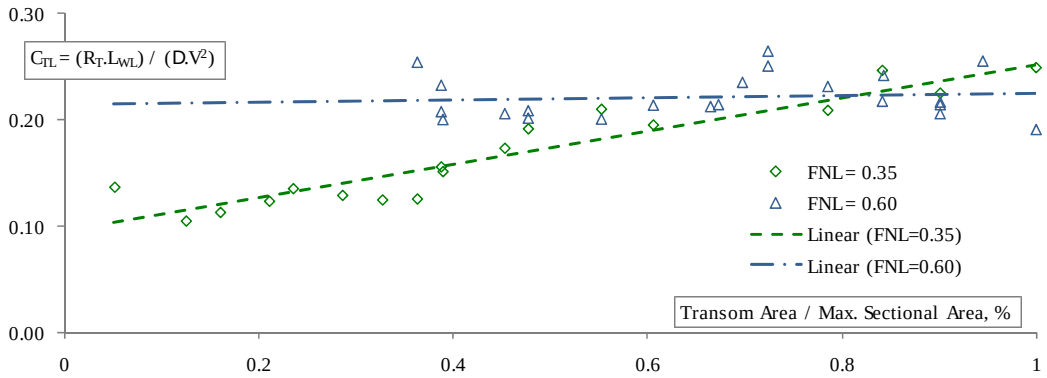

Fig. 2. Dependency of resistance (in the form of C_{TL}) on the immersed transom area at a Froude number of 0.35.

3.4 Trim Control

Additional means to provide lift in the aft part of the hull are transom wedges and flaps, as well as interceptors. In the experience of the authors especially an interceptor is very effective in improving the over-all resistance by reducing running trim. In Fig. 1, the dotted line shows typical results of tank tests with a semi-displacement hard chine hull, with and without interceptor. In the primary resistance hump, a resistance reduction of about 7 to 10% is achieved. Transom wedges are often as effective but these are only optimum at one particular speed. An adjustable interceptor can be made suitable for all speeds.

3.5 Spray Rails

Spray rails are commonly used on semi-displacement yachts. Besides the hydrodynamic advantages, i.e. providing additional lift in the forward part of the hull, positively influencing resistance above certain speeds (Bailey 1974) and decreasing the wetted surface area of the hull by breaking the spray sheet of the bow wave, they are also practical in keeping the deck dryer and avoiding spray to sweep over the deck in beam winds.

3.6 Bulbous Bow

The bulbous bow has been a common feature on displacement hull forms for improving efficiency since the 1960s. Although at first difficult to design, nowadays, by means of optimization techniques using CFD methods, the designer has a much better grasp on the optimum hydrodynamic shape of a bulbous bow. Bulbous bows have a positive effect on the pressure resistance of the fore body as well as on wave wash and the ship waves, in exchange for an increase in wetted surface area. Typical gains in resistance are around 15% in the displacement speed range.

Bulbous bows are commonly used up to the hull speed or slightly over. Experiments carried out by VOA indicate that bulbous bows can also be applied at semi-displacement speeds. Recent tests on a motor yacht of about 44 meter in length have shown that, for this particular yacht, applying a bulbous bow is effective to at least $F_{N,L} = 0.55$, see Fig. 3. When extrapolating the test data, it is found that improvements can be expected up to $F_{N,L} = 0.65$. In Fig. 4 photographs are shown of model tests with and without a bulbous bow at $F_{N,L} = 0.55$. Here, the reduction of the bow wave height as well as a lower running trim due to the bulbous bow can be seen.

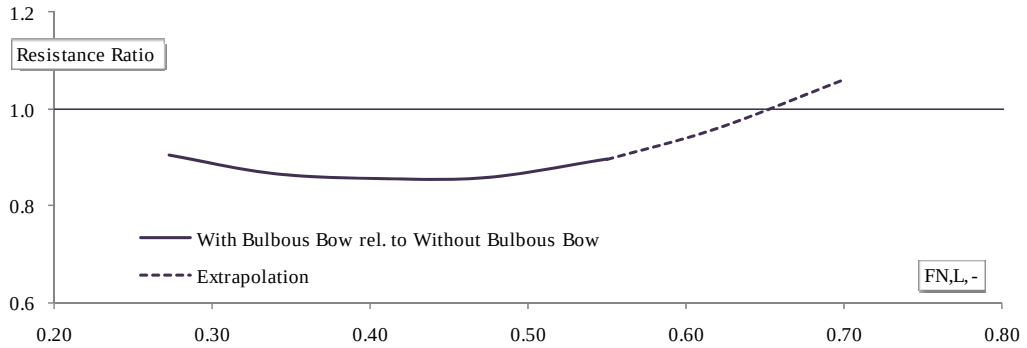

Fig. 3. Tank test results for a 44m motor yacht with and without bulbous bow.

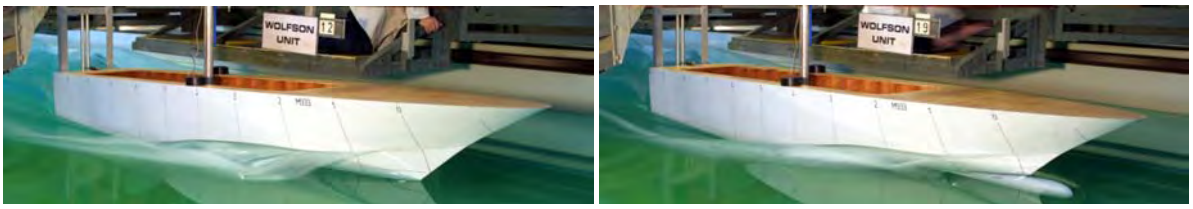

Fig. 4. Model at $F_{N,L} = 0.55$ without bulbous bow (left) and with bulbous bow (right).

4. BULBOUS BOW OPTIMIZATION

4.1 Automatic Hydrodynamic Optimization

At FutureShip GmbH / Fluid Engineering (FS) the hydrodynamic hull optimization task is addressed by a most efficient automatic design and optimization workbench. Applications in the marine sector are broad, besides motor yachts, automatic hydrodynamic optimization was successfully applied by FS in many projects, e.g. to merchant ships like container carriers, bulkers, but also to specialized crafts or high performance sailing yachts. Examples are given, e.g. in Heimann and Harries (2003), Dudson and Harries (2005), Harries et al. (2007), Hochkirch and Bertram (2009).

Since the whole optimization design loop needs to work without user interaction, the interfacing between different tools (e.g. the geometry modeler and the CFD tool) requires much care to ensure a smooth workflow. FS's typical workbench for automatic hydrodynamic optimization, compare Hochkirch and Bertram (2009), is composed of a form-parametric hull geometry modeling and variation instance, FRIENDSHIP Framework (Abt and Harries 2007),

feeding the FS-Equilibrium analyzing the equilibrium conditions of floating bodies in six degrees of freedom, including damage stability and maneuvering, and the state-of-the-art nonlinear free surface Rankine panel flow code FS-Flow. FS-Flow computes the wave resistance either by integrating the pressure over the wetted surface of the hull or from a wave pattern analysis which proved to be a robust analysis method, Heimann et al. (2008). Modern Rankine panel codes are the standard tool of choice to assess wave making and support bulbous bow design, Bertram (2000). The whole process is controlled by the FS-Optimizer, a generic optimization toolkit, for simple set-up of tailored applications, combining a selection of arbitrary analysis, applying a variety of methods for designs space exploration and formal optimization, including advanced multi-objective algorithms and constraints handling. The program can run in unlimited threading mode to make full use of parallel computing environments, like high performance computing clusters. Details to the FS in-house tools are given in FutureShip/Fluid Engineering (2009).

4.2 Bulbous Bow Optimization

In this section, the bulbous bow optimization for a 47 meter motor yacht carried out recently by FS for VOA is presented.

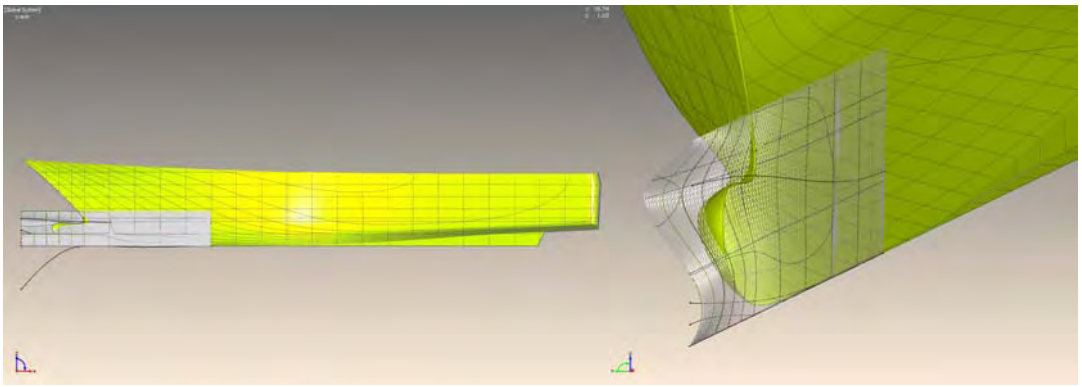

Fig. 5. Paramterized deltaSurface patch for variation of the bulbous-bow and entrance fairing region

Parametric hull design has been a powerful modeling technique during the last decade. Instead of describing the hull shape properties by a large network of lines and points, requiring a lot of manual work, the parametric modeling approach employs so-called high-level form descriptors which describe characteristic properties, e.g. of the sections by means of longitudinal distributions so called ‘meta-curves’. FS’s preferred technique builds B-spline curves from selected properties. These can be described directly, differentially or even by integral formulations. The vertices of the final spline are then automatically placed to ensure a fair distribution of the property required. A typical example is the sectional area curve of a hull where the integral value reflects the required buoyancy.

For the automatic variation of the baseline bulbous bow – entrance region of the 47 meter motor yacht, a so called deltaSurface patch was developed and parameterized within the FRIENDSHIP Framework. The deltaSurface patch covers the whole bulbous bow and entrance fairing region with smooth transition longitudinally at section 2.5 and girthwise at half-load water level into the original (baseline) hull. The forward perpendicular point and the stem were kept fixed, see Fig. 5. Eight longitudinal curves (e.g. sectional area, vertical center of area, end tangents in section plane etc.) define the shape of the deltaSurface longitudinally and girthwise, see Fig. 6. The shape of the longitudinal curves themselves is controlled by form parameters, like end positions and tangents, which were selected (partly) as variables in the exploration and optimization analysis. Moreover, two longitudinal curves along the bulbous bow define the length and vertical shift of the bulb. The surface shift itself is determined by the product of the actual local y-value of the deltaSurface and the corresponding local y-value of the initial surface. Finally, the thus determined actual surface

shift is added to the initial surface. In addition, an elongation and vertical shift of the bulbous bow were applied. Examples of the deltaSurface and the resulting hull surface shift are presented in Fig. 7.

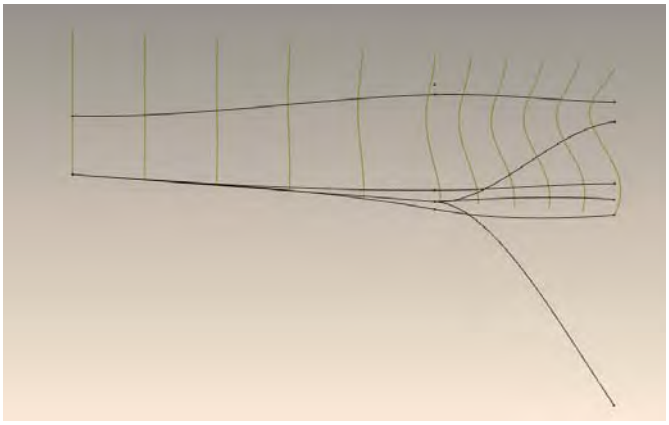

Fig. 6. Longitudinal curves defining the shape of the deltaSurface longitudinally and girthwise

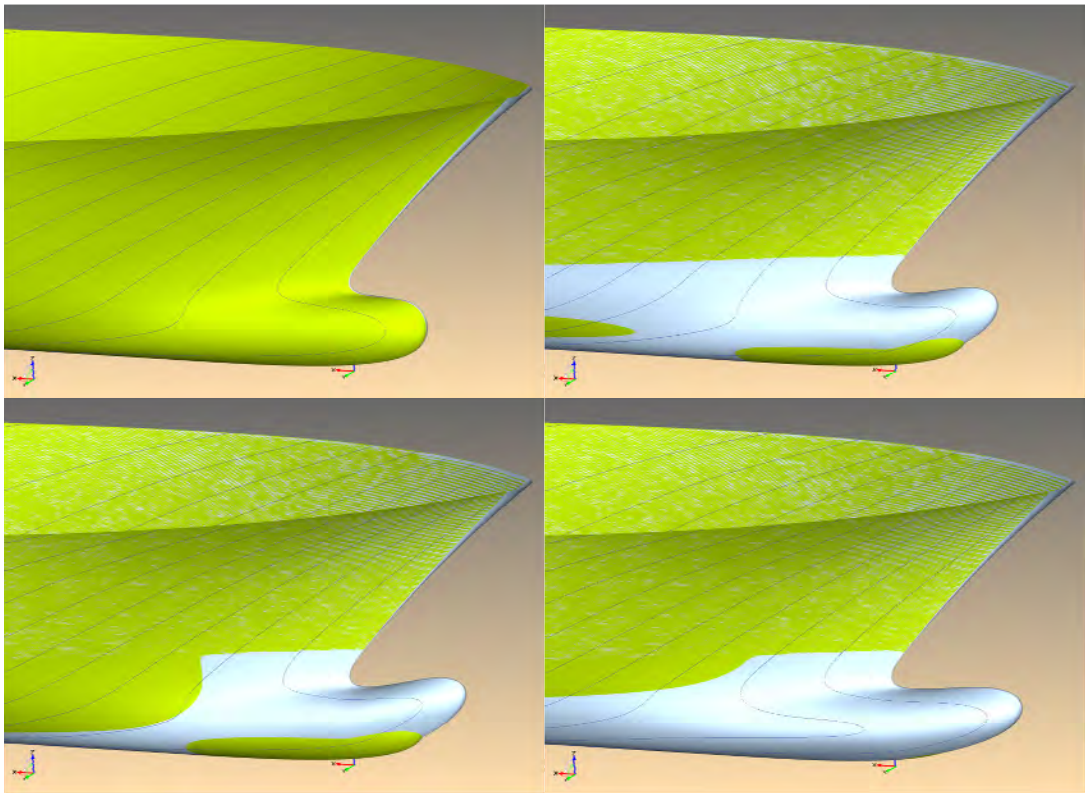

Fig. 7. Effect of variation of the deltaSurface parameters on the bow shape (light grey indicate varied surface regions); upper left: baseline hull to lower right: DoE favored design

In section 3.6 the merit of a bulbous bow at displacement and semi-displacement speeds was discussed. Since motor yachts are supposed to operate most of the time at cruise speed ($F_{N,L} \sim 0.35$.) it is obvious for the designer to optimize the bulb for this very case. However, a constraint or another objective should be that the presence of the bulb is at least not impairing the performance at maximum speed, which is in case of the FDHF around $F_{N,L} = 0.6$. Usually, further objectives are applied, such as hydrodynamic fairing criteria which force a smooth hull surface.

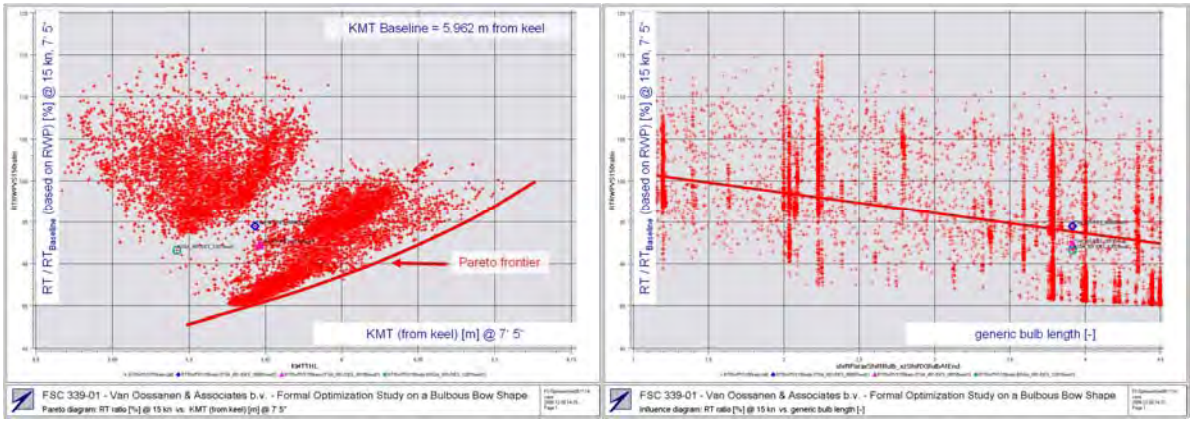

Fig. 8. Pareto frontier R_T vs. KMT (left) and Influence diagram R_T vs. bulb length (right)

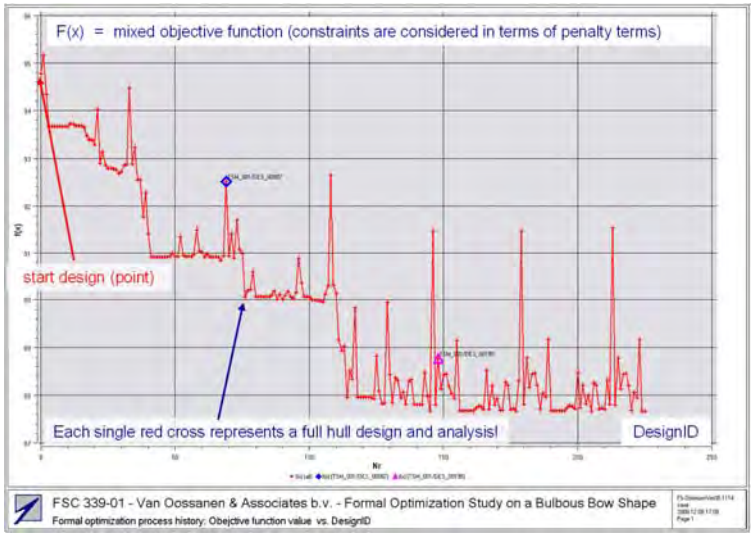

Fig. 9. Deterministic optimization history (Tangent Search Method)

For the 47 meter motor yacht the optimization workbench was established by FS on the basis of the deltaSurface patch and the workbench outlined in 4.1. About thirty free variables, i.e., the form parameters setting up the deltaSurface were selected for optimization. The total resistance at the cruise speed of 15 knots was applied as main objective function. Moreover, the displacement, L_{OA}, the center of buoyancy, the initial stability and the forward perpendicular as a hard point were considered in terms of constraints.

The total resistance is predicted on the basis of the non-viscous resistance components from the FS-Flow CFD simulation and an estimate of the viscous components by the ITTC method, which was based on local flow properties from CFD. Alternatively, the viscous components may be estimated in FS-Flow by an accompanying boundary layer computation. While the integral resistance values are only indicative – depending on the case in question – it is commonly agreed that design rankings are correct with good accuracy if design modifications are limited to the forward half of the ship. This has been confirmed in numerous optimization projects carried out by FS.

At first a comprehensive design space exploration was conducted providing a DoE (Design of Experiments) table. The $\Re^N$-design space was regularly sampled by multi-objective deterministic (NSGA: Non-dominated Sorting Genetic Algorithm) and stochastic exploration sequences (SOBOL: Stochastic non-clustering low-discrepancy sequence), thus generating and successfully analyzing about 24.500 hull variants in total. As a result, the designer is equipped with a most valuable design instrument, a set of so-called Pareto diagrams, which represent the Pareto frontier(s); i.e., the set of non-dominated solutions (hull form designs) revealing the best achievable trade-off between the concurring objectives and/or constraints, e.g. Fig. 8. left. Moreover, influence diagrams can be deduced showing the effect of a specific

form parameter variation on the objective function. For example Fig. 8, right shows the influence of the bulb length on total resistance. In case of the 47 meter motor a protruding bulb is favored.

Finally the DoE database was searched for promising hull variants which were subsequently utilized as starting points for focussed deterministic searches (TSM: Tangent Search Method). A process history is shown in Fig. 9.

In Fig. 10 to Fig. 12 the results of the bulbous bow optimization for the 47 meter motor yacht are shown. In Fig. 11 and 12 the influence of the optimized bulbous bow on the bow wave can be clearly seen. This particular optimization exercise lead to a substantial 8 to 10% reduction in total resistance relative to the non-optimized bulbous bow, as predicted by CFD calculations utilizing the FS-Flow Panel code. A similar optimization was used for the bulbous bow of the Fast Displacement Hull Form.

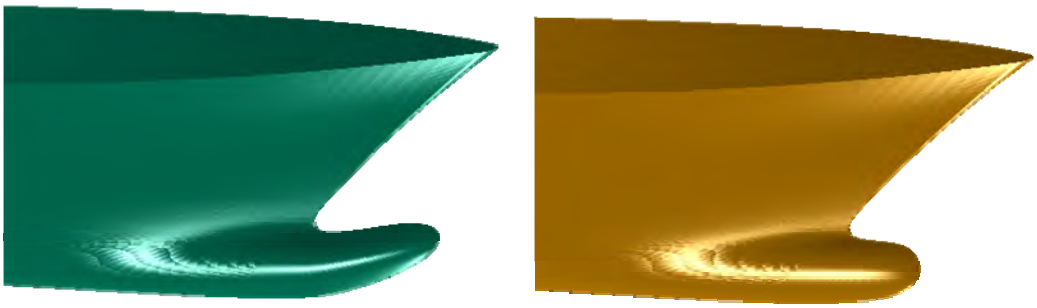

Fig. 10. Rendered views of the bulbous bow on a 47 metre motor yacht before (right) and after (left) a formal optimization

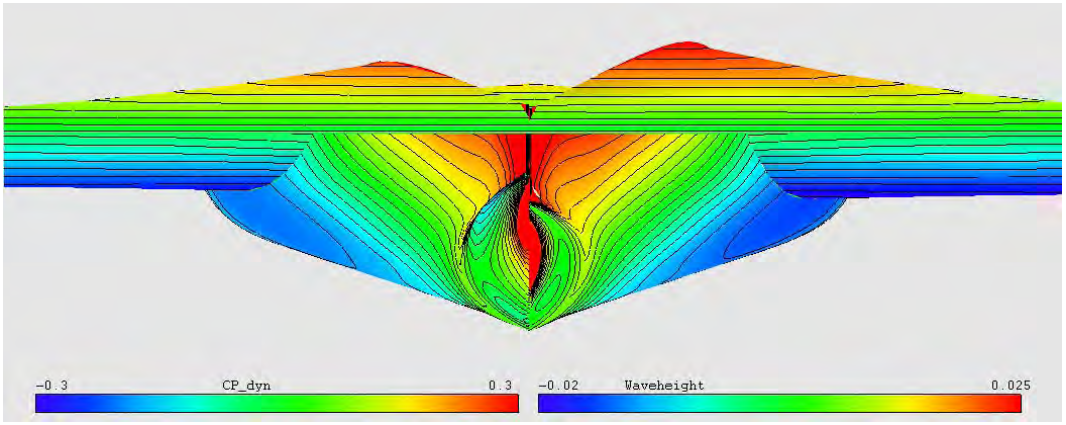

Fig. 11. CFD results for the bulbous bow optimization (dynamic pressure and wave height); left: optimized bulbous bow, right: bulbous bow before optimization

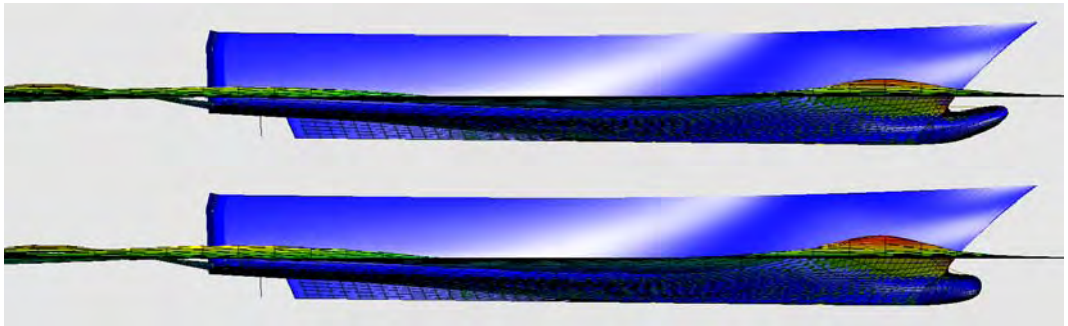

Fig. 12. Wave profiles along the optimized bulbous bow (top) and the bulbous bow before optimization (bottom)

5. ANALYSIS

5.1 Reference Vessels and Resistance Data

As an example for this paper, the design of an all-aluminium semi-displacement motor yacht of about 45 metres in length over-all has been adopted. The length-beam ratio is to be 5.2 and the length-displacement ratio is 6.25. The speed range is from 13 knots for the cruising speed and 24 knots for the maximum speed.

A hard-chine semi-displacement hull form, of which tank test data and CFD results are available, as well as the equivalent hull form from the NPL series, were selected as reference hulls, see Fig. 13. These hull forms have the same length, length-beam ratio and length-displacement ratio.

For the equivalent FDHF, CFD calculations have been carried out using the RANSE code ISIS-CFD (e.g. Deng et al. 2005 and 2006), developed by Ecole Centrale de Nantes which is part of the FINE/Marine package, as made available by Numeca, as well as the FS-Flow Panel Code, as described previously. The results obtained from ISIS-CFD have been extensively validated by means of numerous tank tests, which validation included the selected hard chine reference vessel. All data are for the bare hull forms, with a correction added to the friction coefficient of 0.0002 to account for hull roughness effects for the vessel on trials.

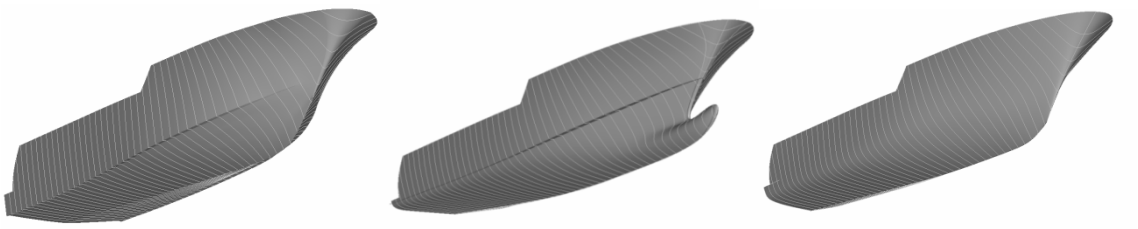

Fig. 13. Selected hull forms for the analysis: a hard-chine semi-displacement vessel (left), the equivalent Fast Displacement Hull Form with bulbous bow (middle) and the corresponding NPL Series Hull Form (right).

5.2 Comparison of Hull Resistance

Resistance values, made non-dimensional by means of C_{TL}, are shown in Fig. 14. The FDHF is here compared to the reference hard chine hull and the corresponding NPL form. The shaded areas indicate typical values of similar displacement and semi-displacement models tested in the towing tank.

For the cruising speed, chosen here as 13 knots and corresponding to $F_{N,L} = 0.34$, it can be seen from the ISIS-CFD results that the FDHF performs equal to the typical displacement hull form, but is significantly better than the average semi-displacement hull form with 40% less hull resistance. Compared to the NPL reference hull, the FDHF also performs better, with a smaller but still significant margin. At a speed corresponding to $F_{N,L} = 0.60$ (i.e. 23.3 knots), the FDHF has over 15% less drag than the equivalent Hard Chine form. The performance of the FDHF at this speed is close to the NPL hull.

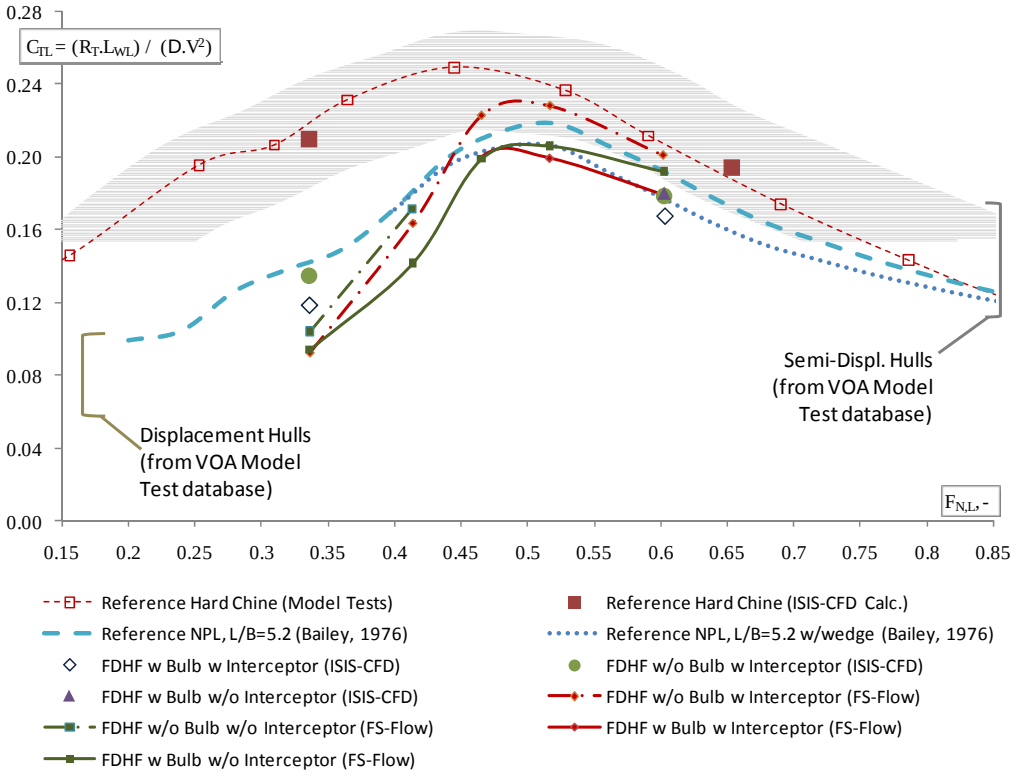

Fig. 14. C_{TL} values for the FDHF, reference Hard Chine and NPL Round Bilge Hull Form.

5.3 Effect of the Bulbous Bow

FS-Flow results as well as the ISIS-CFD results, as shown in Fig. 14 for the FDHF with and without bulbous bow show the influence of the bulbous bow in the displacement speed range, and ISIS-CFD results show the influence at $F_{N,L} = 0.34$ and 0.60. Although the absolute value of the calculated resistance values differ between the two codes, the relative effect of the bulbous bow corresponds and is in line with previous results. The influence of the bulbous bow on the resistance can also be found in Fig. 15. Around the hull speed, $F_{N,L} \approx 0.45$, the bulbous bow is most effective. At higher speeds the efficiency decreases but still improves the resistance values by an appreciable margin. In Fig. 16 the wave profile and wave elevations can be seen for the cruising speed case, as results from ISIS-CFD.

It is to be noted that the actual bulbous bow shape of the FDHF has not been formally optimized using the approach explained in Chapter 4, although results from previous optimizations (at displacement speed!) have been used as inspiration for the design. Future work is to point out the additional gains obtained from an optimization for the bulbous bow shape of the FDHF.

5.4 Effect of the Interceptor

The effect of the interceptor has been determined from ISIS calculations for the Parent FHDF, at $F_{N,L} = 0.60$, with and without interceptor, see Fig. 17 (the points at $F_{N,L} = 0.60$, for the FDHF without bulbous bow, with interceptor, coincides with the FDHF with bulbous bow, without interceptor). The interceptor (set at 50mm) reduced the running trim angle by about 1 degree, from 1.69° to 0.73°. This change in running trim caused a reduction in resistance of about 7%. From Fig. 17, it can be seen that, with the interceptor deployed, the bow wave climbs steeper up to the spray rail. The rising of the stern by the lift force generated by the interceptor caused the transverse stern wave to decrease, both in height and steepness. This latter effect is the major reason for the decrease in resistance. In Fig. 14 also FS-Flow

results are given for the FDHF with and without bulb and both with and without interceptor. The predicted values for the dynamic trim and sinkage correspond very well between FS-Flow and ISIS.

It is to be noted that for the NPL series, a transom wedge of about 10 degrees gives a resistance reduction of about 8% (Bailey 1976) and results in about the same resistance as the FDHF without bulbous bow, see also Fig. 14.

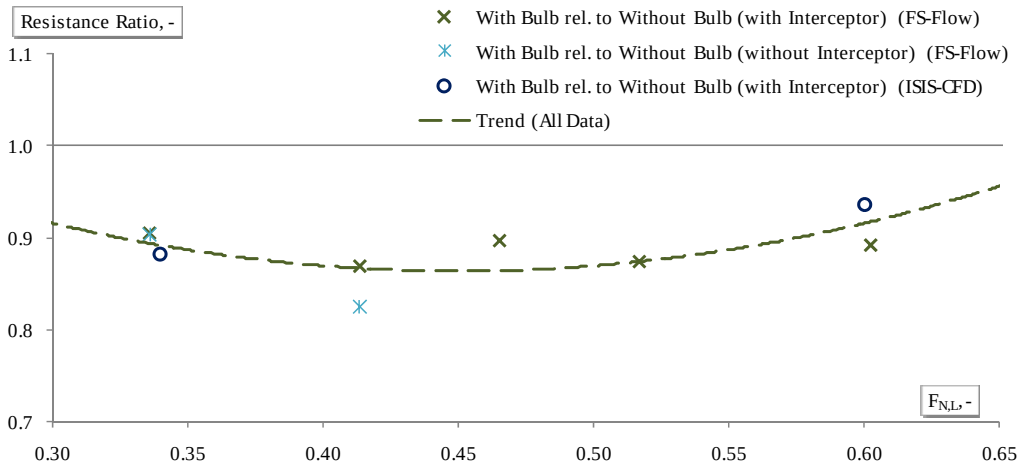

Fig. 15. Resistance ratio of the FDHF with bulbous bow, relative to the FDHF without bulbous bow, by using FS-Flow and ISIS-CFD.

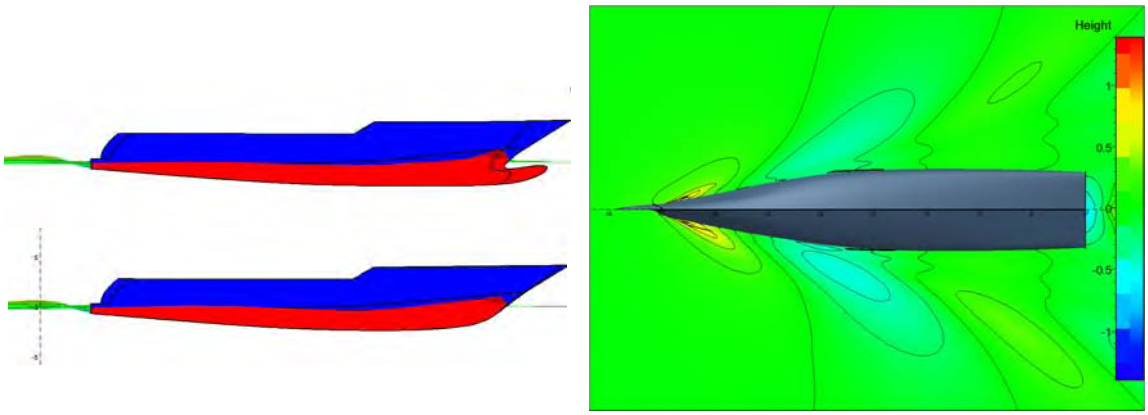

Fig. 16. Comparison of wave profiles (left) and wave elevations (right) for the Parent FDHF, with bulbous bow (top) and without bulbous bow (bottom) at $F_{N,L} = 0.34$.

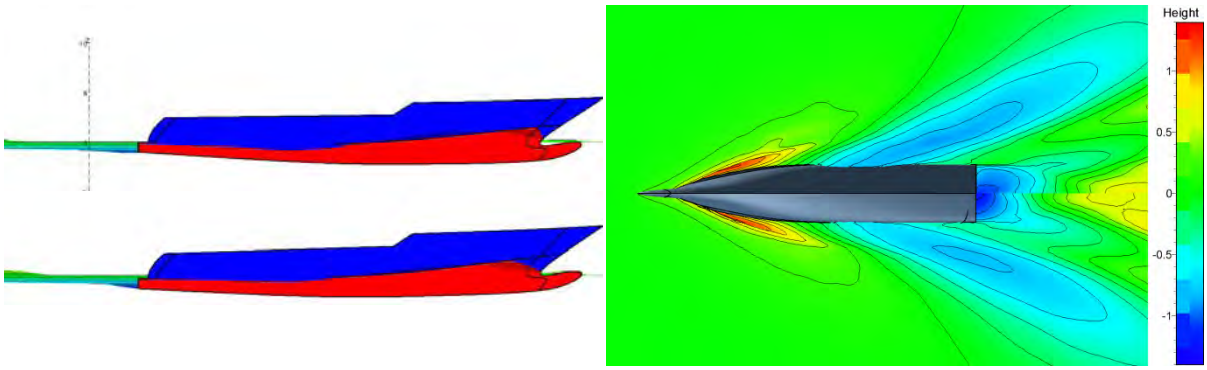

Fig. 17. Comparison of wave profiles (left) and wave elevations (right) for the Parent FDHF, with interceptor (top) and without interceptor deployed (bottom) at $F_{N,L}=0.60$.

5.5 Comparison of Powering Performance

Using normal power prediction techniques, using the resistance information as obtained from the various calculations, a trial prediction has been made for the reference hard chine vessel and the equivalent FDHF, of which the results can be seen in Fig. 18. Here, an optimum propeller with a diameter of 1.8m has been selected at maximum power and RPM for a given engine (2x 1920kW @ 1970RPM). Using a fuel capacity of 50 tonnes, and assuming a 5% reserve, the range has been determined using the engine's consumption characteristics for the actual propeller curves. The calculations show that the FDHF improves top speed by almost 2 knots and improves the range at the cruising speed by over 1500 nautical miles.

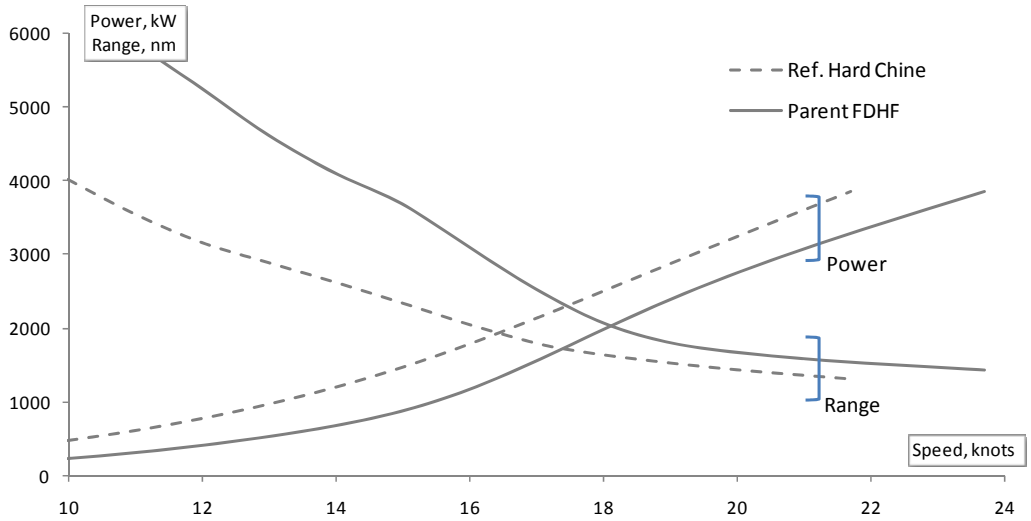

Fig. 18. Comparison of Power and Range for the FDHF and the reference hard Chine hull.

6. APPLICABILITY AND PRACTICAL CONSIDERATIONS

6.1 Stability

It is well-known that a round bilge hull has a lower initial stability than a comparable hard chine hull. In order to assess the stability characteristics of the FDHF, a limiting KG calculation has been carried out, for the Parent FDHF as well as for the Hard Chine reference vessel. For this analysis, the MCA Large Yacht Code 2 stability requirements have been used. The results indicate that the limiting KG curve for the FDHF is lower by about 5 to 7% of the depth (about 20 to 25 cm) compared to the limiting KG curve for the hard Chine hull form, see Fig. 19. This is identified to be especially due to the "weak" bilges of the FDHF, causing a reduction in the metacentric radius at moderate angles of heel

It is to be noted that the limiting KG of the FDHF as presented should not invalidate the applicability of the FDHF concept for a motor yacht, although for yachts with relative voluminous and stretched superstructures, the stability might become critical, in which case the beam will need to be increased.

In order to develop a yacht with a similar stability range as the hard chine yacht, an 8% increase in beam of the FDHF is necessary. The limiting KG curve for this widened form is also shown in Fig. 19. In order to quantify this widening in terms of resistance, an additional CFD calculation has been carried out at $F_{N,L} = 0.6$ with the same interceptor setting as for the Parent FDHF. This showed only a marginal increase in resistance (by about 1.5%). The same observation is made for the NPL series, where a similar reduction of the length-beam ratio results only in a 0.7% resistance increase.

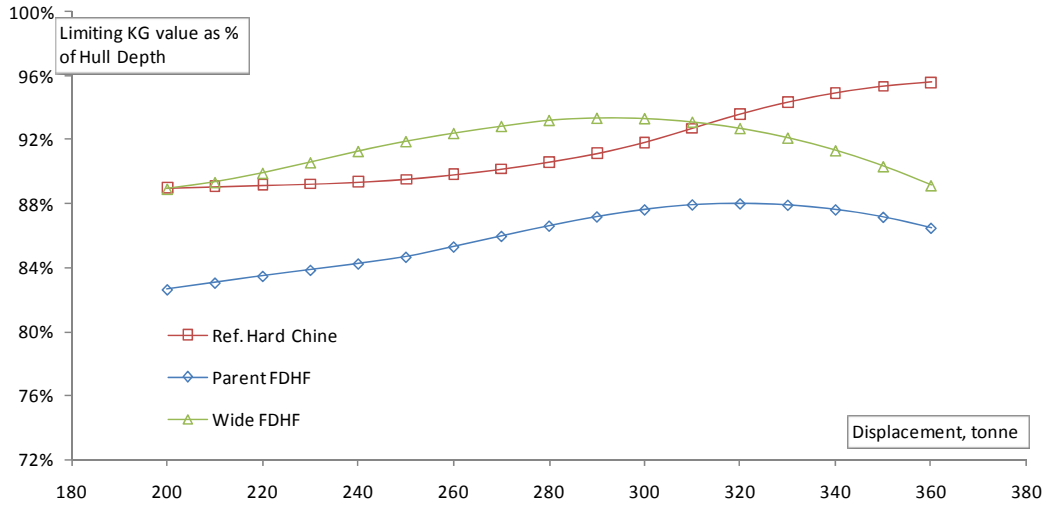

Fig. 19. Results of limiting KG analysis for the reference hard chine vessel and the parent FDHF, as well as for a widened FDHF model.

6.2 Interior Floor Space

The FDHF has a rather fine waterline entry compared to the hard chine reference vessel, as is common for most round bilge hulls compared to hard chine hulls. If the lack of floor area (especially in the fore body where the crew is usually situated) is critical, the designer has the option to widen the hull entirely, as discussed in the previous paragraph, or widen only the forebody and shorten the length of entrance of the waterline. The effects of this latter option are yet to be fully analyzed.

6.3 Build Costs

For a steel or aluminium hull, the costs of work preparation for round bilge hulls are slightly higher than for a hard chine yacht. This is due to the cost of the additional bending of plates and the production of the associated bending moulds. Considering the reduced fuel consumption and perhaps the reduced investment cost of the main engines, these additional costs will be minor in comparison. Many factors, such as country of build, steel and oil prices, usage and load profile, etc., influence these points. It is expected that for the FDHF these additional cost will be outweighed by the advantages the concept holds.

7. CONCLUSION AND PERSPECTIVE

The concept of the Fast Displacement Hull Form, combining a round bilge hull, a small immersed transom area, a bulbous bow, trim control and spray rails is shown to be favourable from a resistance point of view when compared to results of model tests and CFD calculations for typical (hard chine and round bilge) semi-displacement motor yachts. At displacement speeds resistance values of the FDHF are comparable to displacement yachts and show a major improvement relative to typical semi-displacement motor yachts. At semi-displacement speeds it is shown that a bulbous bow as well as trim control improve the resistance.

The formal optimization method as discussed, has proven to be a valuable method to design bulbous bows, as well as for general hull form optimization.

Future work to be carried out, such as a further optimization of the bulbous bow, further hull form refinement, optimization of the interceptor settings at each speed separately, will most likely entail further improvements in resistance values for the FDHF.

If the FDHF is found to possess slightly less stability than a comparable hard chine hull, this may be solved by a widening of the hull without a large resistance penalty. In case of a lack of interior space and floor area a similar approach may be used.

References

Abt, C. and Harries, S. (2007). 'A new approach to integration of CAD and CFD for naval architects', 6th COMPIT, Cortona, pp.467-479, http://www.ssi.tu-harburg.de/doc/webseiten_dokumente/compit/dokumente/compit2007_cortona.pdf.

Bailey, D. (1974). 'Performance Prediction – Fast Craft'. Royal Institution of Naval Architects, RINA Occasional Publications No. 1.

Bailey, D (1976). 'The NPL High Speed Round Bilge Displacement Hull Series'. Maritime Technology Monograph, No. 4.

Bertram, V. (2000). 'Practical Ship Hydrodynamics', Butterworth & Heinemann

Blount, D.L. (1995). 'Factors Influencing the Selection of Hard Chine or Round-Bilge Hull for High Froude Numbers', Royal Institution of Naval Architects, Proceedings of FAST 1995.

Blount, D.L. and McGrath, J. (2009). 'Resistance Characteristics of Semi-Displacement Hull Forms'. Royal Institution of Naval Architects, Proceedings of the Symposium on the Design, Construction and Operation of Super and Mega Yachts, Genoa, Italy.

Deng, G.B., Guilmineau, E., Queutey, P., Visonneau, M. (2005). 'Ship Flow Simulations with the ISIS-CFD Code'. CFD Workshop Tokyo 2005, T. Hino (Ed.), Tokyo, pp.474-482.

Deng, G.B., Queutey, P., Visonneau, M. (2006). 'A Code Verification Exercise for the Unstructured Finite Volume CFD Solver ISIS-CFD'. ECCOMAS-CFD, E. Oñate, P. Weeseling, J. Priaux (eds).

Doctors, L.J. (2006). 'Influence of Transom-Hollow Length on Wave Resistance'. International Workshop on Water Waves and Floating Bodies 21, Loughborough, UK, 2006.

Dudson, E. and Harries, S. (2005). 'Hydrodynamic fine-tuning of a pentamaran for high-speed sea transportation services', Int. Conf. Fast Sea Transportation (FAST 2005), St. Petersburg, http://www.fsopt.com/downloads/2005_PaperDudsonHarriesFinal.pdf.

FutureShip / Fluid Engineering (2009). 'FS-FLOW, FS-SHALLOW, FS-WAVES, FS-OPTIMIZER, FS-EQUILIBRIUM Release and Users Manuals, Rel.09x', FutureShip GmbH, http://www.fsopt.com.

Harries, S., Hinrichsen, H. and Hochkirch, K. (2007). 'Development and application of a new Form Feature to enhance the Transport Efficiency of Ships', Jahrbuch der Schiffbautechnischen Gesellschaft, http://www.fsopt.com/downloads/2007_STGpaperInSAC_HaHiHo.pdf.

Heimann, J. and Harries, S. (2003). 'Optimization of the Wave-Making Characteristics of Fast Ferries', 7th Int. Conference on Fast Sea Transportation (FAST 2003), Ischia (Gulf of Naples), Italy, http://www.fsopt.com/downloads/2003_FAST_HeimannHarries.pdf.

Heimann, J., Hutchinson, B. L. and Racine, B. J. (2008). 'Application of the Free-Wave Spectrum to Minimize and Control Wake Wash', SNAME Annual Meeting & Expo, Houston, http://www.sname.org/AM2008/papers/049.pdf.

Hochkirch, K. and Bertram, V. (2009). 'Slow Steaming Bulbous Bow Optimization for a Large Containership'. 8th COMPIT, May 10th - 12th, Budapest, http://www.ssi.tu-harburg.de/doc/webseiten_dokumente/compit/dokumente/compit2009.pdf.

Keuning, J.A. (1984). 'Comparison of the Resistance and Motions in Waves of a Round Bilge and Hard Chine Model of a High Speed Displacement Ship'. Report of the Hydromechanics Laboratory, Delft University of Technology, No. 612, 1984.

Telfer, E.V. (1963). 'The Design presentation of Ship Model Resistance Data'. North East Coast Institution of Engineers and Shipbuilders, Transactions Vol. 79.